

Formulation and Optimization of Aripiprazole-Loaded Nanostructured Lipid Carriers for Nose-to-Brain Delivery

Layla Albaqshi^{1,*}, Amanjot Singh², Shahzad Khan³, Manish Kumar⁴, Jagpreet Kour⁵, Shinu Pottathil³, Bandar Aldhubiab¹, Abhishek Tiwari⁶, Anroop B Nair¹

¹Department of Pharmaceutical Sciences, College of Clinical Pharmacy, King Faisal University, Al-Ahsa, SAUDI ARABIA.

²Department of Pharmaceutics, M. M. College of Pharmacy, Maharishi Markandeshwar (Deemed to Be University), Ambala, Haryana, INDIA.

³Department of Biomedical Sciences, College of Clinical Pharmacy, King Faisal University, Al-Ahsa, SAUDI ARABIA.

⁴Department of Pharmaceutics, ISF College of Pharmacy, Moga, Punjab, INDIA.

⁵Department of Pharmaceutics, School of Pharmaceutical Sciences, CT University, Sidhwan Khurd, Ludhiana, Punjab, INDIA.

⁶Department of Pharmaceutical Sciences, Faculty of Pharmacy, IFTM University, Moradabad, Uttar Pradesh, INDIA.

ABSTRACT

Background: Low bioavailability, highly variable blood levels and poor clinical efficacy of Aripiprazole (ARP) are primarily linked to its hydrophobic nature. This investigation focused on the formulation of ARP loaded Nanostructured Lipid Carriers (NLCs) incorporated in thermoreversible *in situ* intranasal gel for brain delivery. **Materials and Methods:** The high-speed homogenization method was used to formulate ARP loaded NLCs. A factorial design was utilized to optimize the particle size, entrapment efficiency and drug release of NLCs by selecting Tween 80 as a surfactant and stearic acid and castor oil as solid and liquid lipids, respectively. The ARP loaded NLCs thermoreversible *in situ* gel was fabricated using Poloxamer 407 as a phase transition agent and carbopol 940 as a mucoadhesive agent. The gel formulation was characterized for various pharmaceutical properties and nasal ciliotoxicity. **Results:** The optimized NLC (Z7) had nano size (~150 nm), good entrapment efficiency (~93%) and higher drug release (~75% in 12 hr). The formulated thermoreversible *in situ* gel (Z2 G) showed ideal gelling temperature, gel strength, and pH suitable for nasal use in addition to steady drug release and greater permeation. The toxicity study data revealed that the gel is safe for intranasal application. **Conclusion:** The prepared thermoreversible *in situ* gel of ARP loaded NLCs showed excellent potential for intranasal use and can be a feasible alternative to oral therapy in schizophrenia.

Keywords: Schizophrenia, Aripiprazole, Optimization, Poloxamer, Thermoreversible gel, Intranasal.

Correspondence:

Ms. Layla Albaqshi

Department of Pharmaceutical Sciences,
College of Clinical Pharmacy, King Faisal
University, Al-Ahsa-31982, SAUDI ARABIA.
Email: 220010553@student.kfu.edu.sa

Received: 08-11-2023;

Revised: 28-12-2023;

Accepted: 09-01-2024.

INTRODUCTION

Schizophrenia often entails phases of remission and relapse due to its incapacitating and chronic psychotic nature, which significantly affects the patient's capacity to function in social situations.¹ This chronic disorder typically manifests in late adolescence or early adulthood and has affected roughly 24 million population globally during the last decade. World Health Organization projects that 20% of Indians will experience certain types of mental disease by 2025, while the ICMR (Indian Council of Medical Research) reports that mental disorders are sweeping the globe, including India, at an epidemic rate.² Schizophrenia being a complex endogenous mental illness shows three characteristic symptoms.³ The first category (positive)

symptoms include hallucinations and delusions, as well as notable and dramatic shifts in behavior and mental patterns. The negative signs (second category) include dementia, impaired interpersonal relationships, social detachment, inaction, alolia, fatigue, and a shortage of motivation and responsibility to carry out routine daily tasks, while the third category (disorganized) signs include pronounced deficiencies in spoken and mental memory, alertness, and focus.

Neuroleptics, antipsychotics and heavy tranquilizers are the three broad categories of medications used for the standard treatment of schizophrenia.⁴ The first line of treatment is antipsychotic medication, which is further divided into atypical or 2nd generation antipsychotics such as Aripiprazole (ARP), risperidone, olanzapine, clozapine, paliperidone, etc. Typical or first generation antipsychotics which include drugs such as haloperidol, perphenazine, loxapine, etc.⁵ Second generation antipsychotics are considered as a significant advancement, primarily due to their reduced risk of developing side effects and their expected improvement in efficacy and safety.⁶ In addition,



DOI: 10.5530/ijper.58.2.64

Copyright Information :

Copyright Author (s) 2024 Distributed under
Creative Commons CC-BY 4.0

Publishing Partner : EManuscript Tech. [www.emanuscript.in]

a general movement towards second generation antipsychotics in the management of schizophrenia has been brought about by attributes including superiority in the treatment of cognitive enhancement, enhanced individual tolerability, and experience.⁷

ARP belongs to the quinolinone derivative and is a 2nd generation antipsychotic drug accepted by the US FDA for the management of negative, positive and depressive schizophrenia-related symptoms.⁸ ARP has a unique mode of action and receptor binding profile. It facilitates the antipsychotic effect by acting as a partial agonist at the Dopamine (D2) and serotonin (5-HT_{1a}) receptors while as an antagonist of the 5-HT_{2a} receptor.⁹ Indeed, ARP has a lesser potential to produce additional pyramidal symptoms and seems to be more successful in treating the accompanying adverse signs of schizophrenia. ARP is available commercially as oral tablets, solutions, and intramuscular depot injections. Low oral bioavailability, highly variable blood levels and irreproducible clinical responses of ARP are caused due to the hydrophobic nature and therefore considered as a BCS class II drug.¹⁰ Moreover, it is extensively metabolised in the liver and undergoes P-glycoprotein efflux, which increases the risk of side effects that are dose related, such as hypotension, akathisia, neuroleptic malignant syndrome, QTc prolongation, dry mouth, tremor and high blood sugar (in diabetic patients).^{11,12} Many attempts were reported to enhance the ARP dissolution rate and bioavailability by various approaches¹²⁻¹⁵ including salt formation, prodrugs, solid dispersion, solid lipid nanoparticles, orodispersible films, etc. However, an ideal formulation in oral therapy to provide adequate clinical efficacy is still unmet. This low efficiency is well correlated to the limited permeability of drugs in CNS disorders to cross the blood brain barrier.¹¹ Thus, it seems the clinical efficacy of ARP is not just limited to its solubility but is equally influenced by its inability to transport through the endothelium, the main barrier to brain delivery. To this end, alternative ways of administration such as the intranasal route can be more effective.¹⁶

With the advancement of nanotechnologies, a number of nanocarriers have emerged that have enormous potential for improving drug penetration through the BBB and targeting brain cells with minimal adverse effects.¹⁷⁻²⁰ Among the drug targeting approaches, nose to brain drug delivery has gained wide attention recently as a less invasive way to deliver the drug to brain while avoiding the liver first pass effect and the blood brain barrier.^{16,21} Due to the highly vascularized nasal epithelium and the unique way that the olfactory nerve system connects the brain, drugs can reach the target region, or brain tissue, very quickly.²² Various categories of drug carriers are developed and evaluated for their potential for intranasal delivery.^{17,23} An attempt to deliver ARP through intranasal using poly(caprolactone) polymeric nanoparticles was recently reported.¹¹

The great potential of drug loaded Nanostructured Lipid Carriers (NLCs) over other lipid containing nanoformulations

in the therapy of various neurological conditions by intranasal route has been described in the literature.²⁴⁻²⁸ Thus, NLCs were chosen as cargo to transport ARP to the brain area. However, gel formulations are considered a suitable delivery vehicle to enhance the retention, reducing post-nasal drip and permeation of nanocarriers through the intranasal route for effective CNS delivery.^{24,29,30} In this regard, *in situ* gelling systems possess several advantages over conventional nasal administration systems such as improved patient adherence, enhanced drug retention, uniformly spread to the mucosal tissue, etc.³¹ Considering all the above facts, the objective of this study was to develop and evaluate thermoreversible *in situ* gel containing ARP loaded NLCs for possible nose to brain delivery.

MATERIALS AND METHODS

Chemicals

ARP was purchased from Almon Industries, Vithaludyog Nagar, Gujarat, India. Poloxamer 407 was acquired from Glenmark Pharmaceuticals, Baddi, India. Stearic acid and castor oil were acquired from Qualikems, New Delhi, India. Tween 80, carbopol 940 and Polyvinylpyrrolidone (PVP) K30 were procured from Central Drug House Ltd, New Delhi, India. All solvents and other reagents used were of high analytical grade and were procured from local distributors.

Screening of Lipids

The selection of solid/liquid lipids was done based on the preliminary solubility study performed as described previously.³² The solid lipids (carnauba wax, stearic acid, glyceryl monostearate) were heated on a temperature controlled hot plate to a temperature well above its normal melting range before ARP was gradually added. The drug's saturation solubility was considered as the point at which it stopped dissolving in the solid melted lipid. To assess the solubility of ARP in liquid lipids, the equilibrium solubility approach was utilized.³³ Briefly, a surplus amount of ARP was added to the centrifuge tube that contained 1 g of various liquid lipids (oleic acid, paraffin oil, castor oil). The tube was allowed to mix in a thermostatic water bath shaker for 24 hr and 30 min followed by centrifugation (REMI R-4C, Vasai, India) at 10,000 rpm. The supernatant collected was mixed with alcohol to get proper dilution and measured using a UV spectrophotometric technique at 252 nm. The experiment was performed in triplicate.

Formulation of ARP Loaded NLCs

ARP loaded NLCs were formulated using the high speed homogenization technique described previously.³⁴ Liquid lipid and melted solid lipid were combined under constant stirring while maintaining the temperature of the lipid mixture 10-15°C above the melting point. Then the ARP was added to get the homogenous dispersion. The required amount of surfactant was dispersed in pure water to obtain an aqueous phase and the

temperature of the mixture was increased to be similar to that of the lipid mixture. The lipid mixture was gradually added to the surfactant solution using a high speed mechanical agitator (SLISC™, Vasai, India) at 6000 rpm for 45 min followed by instant cooling to form NLCs.

Experimental Design

A 3² full factorial was utilized to design the formulation of ARP loaded NLCs. Solid lipid and liquid lipid ratios (X_1 , 1:1, 2:1, 4:1) and concentration of surfactant (X_2 , Tween 80; 1, 2 and 3%) were identified as independent variables. On the other hand, particle size (Y_1), % entrapment efficiency (Y_2) and % Cumulative Drug Release (CDR) at 12 hr (Y_3) were selected as dependent variables as described in an earlier study³⁵ and the details are shown in Table 1. Batches Z1-Z9 were created by changing two distinct components at three different stages, and Design Expert software version 13 (Stat-ease, Inc., Minneapolis, USA) was used to statistically estimate the dependent variables using Analysis of Variance.

For each response, a polynomial equation was generated and the effect of the solid to liquid lipid ratios and surfactant amount on the dependent variables was also determined using 3D response surface methodology.³⁶ The best (optimized) nanoparticle was identified based on the small particle size, high effectiveness of entrapment and greater % of CDR.

Particle Size

The hydrodynamic diameter of prepared NLCs was calculated using the dynamic light scattering technique with the help of Zetasizer (Malvern Instruments Ltd., Worcestershire, UK). Samples of NLC were taken in a transparent glass cuvette and placed in the cavity and the measurement was carried out at 90° scattering angle.³⁷

Entrapment Efficiency (%)

For the measurement of the entrapment efficiency of ARP loaded NLCs, the prepared formulation was centrifuged at 10000 rpm for 45 min at 4°C in a cooling centrifuge. The supernatant layer containing the free drug was separated and quantified using UV spectroscopy at 252 nm after appropriate dilution. The entrapment efficiency was determined according to the equation mentioned earlier.³⁸

ARP Release from NLCs

The release of ARP from the NLCs was carried out in a Franz diffusion cell with dialysis membrane (Hi Media Ltd., Mumbai, India) as a barrier. The membrane used for the separation of the donor and receptor had an actual mesh size of 0.22 μm. The formulated NLCs were kept in the donor and the receiver had phosphate buffer (pH, 6.4) with 0.5% Tween 80 (to maintain sink).³⁹ The temperature of the system was set at 37°C. At predetermined intervals, 2 mL of receiver solution was taken and the content of ARP was determined by UV spectroscopy. The ARP release kinetics mechanism was evaluated for various models according to the literature.^{37,40} The experiment was conducted in triplicate.

Differential Scanning Calorimetry (DSC)

Thermo analytical technique (Q20 V24.4 Build 116, Universal V4.5A TA equipment, Newcastle, PA, USA) was used to record the sample's thermogram. The specimen was weighed in an aluminium container and the scanning was done at 25-400°C in an arid nitrogen environment at a 10°C/min heating rate.³⁵

Transmission Electron Microscopy (TEM)

ARP loaded NLCs surface morphology investigations were carried out using a TEM (Hitachi H-7500, Tokyo, Japan) operated at 120 kV. After dilution of the sample (20 times) in deionized water, it was put onto a 400 mesh copper grid coated with copper

Table 1: 3² Full factorial design used for the preparation of aripiprazole loaded nanostructured lipid carriers.

| Formulation Code | Drug | Lipid Ratio X_1 | Tween 80 (%) X_2 | Dependent Variables |
|------------------|--------|-------------------|--------------------|--|
| Z1 | 100 mg | 1:1 | 1 | Particle size (Y_1) |
| Z2 | 100 mg | 2:1 | 1 | |
| Z3 | 100 mg | 4:1 | 1 | |
| Z4 | 100 mg | 1:1 | 2 | % EE (Y_2) |
| Z5 | 100 mg | 2:1 | 2 | |
| Z6 | 100 mg | 4:1 | 2 | |
| Z7 | 100 mg | 1:1 | 3 | % Cumulative drug release at 12 hr (Y_3) |
| Z8 | 100 mg | 2:1 | 3 | |
| Z9 | 100 mg | 4:1 | 3 | |

Table 2: Composition of aripiprazole loaded nanostructured lipid carrier thermoreversible gel batches.

| Formulation Code | Poloxamer 407 (% w/v) | Carbopol 940 (% w/v) | PVP K30 (% w/v) |
|------------------|-----------------------|----------------------|-----------------|
| Z1 G | 25 | 0.2 | - |
| Z2 G | 25 | 0.4 | - |
| Z3 G | 25 | 0.6 | - |
| Z4 G | 25 | - | 0.2 |
| Z5 G | 25 | - | 0.4 |
| Z6 G | 25 | - | 0.6 |

film. The particles were stained using phosphotungstic acid, air dried and viewed at a magnification of 8000 \times .

ARP loaded NLCs Thermoreversible Gel Formulation

The cold technique was implemented in the formulation of thermoreversible *in situ* gel with ARP loaded NLCs.²⁹ The composition of various gel prepared are presented in Table 2. Different quantities of carbopol 940P or PVP K30 were slowly included in the poloxamer 407 dispersion, which was prepared by dissolving poloxamer in cold water by slowly mixing using a magnetic stirrer. The optimized ARP loaded NLC formulation was gradually incorporated into the above dispersion with constant stirring and then left undisturbed for 12 hr and stored at 4°C for 24 hr to completely dissolve the mucoadhesive ingredients.

Evaluation of ARP Loaded NLCs Gel

The prepared gel was checked for pH, gel strength and gelation temperature. A precalibrated pH meter was used to ensure the accuracy of the results. The gel strength was determined by the method reported in the literature.⁴¹ Briefly, the thermoreversible gel (50 g) was placed in a beaker and gelled at 27-36°C using a controlled water bath. A standard weight of 35 g was kept on the surface of the prepared gel and the time necessary for the movement of the object to move down 5 cm was considered as its strength. The gelation temperature and time were determined by the visual inspection method. The gel was kept in a glass tube and the temperature was raised by 1°C. The temperature at which the gel doesn't flow by tilting the glass tube at a 90° angle was observed as gelation temperature and the time as gelation time.⁴² Optimized formulation was chosen based on the clarity, and highest gelling capacity.

Ex vivo Drug Permeation of ARP loaded NLCs Gel

The permeation of ARP loaded NLCs across the membrane was assessed using a standard Franz diffusion cell.⁴³ The goat nose was obtained from the nearby slaughterhouse, kept in a 10% formalin solution and stored at ice cold temperature. Forceps and scissors were used to delicately remove the nasal mucosa, and it was then submerged in Ringers' solution. The nasal mucosa membrane was fixed between the two chambers and the temperature was maintained at 37°C. The donor compartment was placed with

ARP loaded NLC thermoreversible *in situ* gel (Z2 G, 500 mg) equivalent to 10 mg drug or pure drug suspension. Phosphate buffer (pH 6.4, 10 mL) with 0.5% Tween 80 (to maintain sink) was used as the receiver solution. At predetermined intervals, 2 mL of receiver solution was taken, properly diluted and analyzed by spectrophotometry at 252 nm.

Histopathological Study

For the nasal ciliotoxicity study, the goat nasal mucosa was used. Histopathological studies were carried out on three equally cut samples of the nasal mucosa (A, B, and C) that were kept individually on Franz diffusion cells (maintained at a temperature of 37°C). Sample A was untreated and used as a negative control. Sample B was applied with a standard irritant (0.5 mL of isopropyl alcohol) to damage the tissues (positive control) while test sample C was applied with the ARP-loaded NLC *in situ* gel. These mucosal cells were stained using the hematoxylin eosin method after 24 hr of *ex vivo* drug permeation. The tissues were examined by a trained pathologist under high power (400x magnification) using a light microscope (Olympus CX23, Tokyo, Japan).³

Stability Studies

The optimized NLC Z7 was subjected to stability assessment by storing it in a room for three months at standard conditions according to ICH. NLCs were placed in a 5 mL dark vial with a cap. In addition, samples were obtained at the start and end of the three months to determine the physical appearance, % entrapment efficiency, particle size, and % CDR.⁴⁴

RESULTS AND DISCUSSION

Selection of Lipids Based on Solubility Studies

It is vital to screen the lipids to develop NLCs for brain targeting through the nose to brain route to achieve stability as well as required particle characteristics.⁴⁵ In addition, the selection of lipids is equally important as it directly affects the drug loading capacity as well as its release from the NLCs.⁴⁶ Furthermore, the excellent solubility of drugs in NLCs would eventually aid in dose reduction because the entire drug (inside the NLCs) is available for pharmacological effect. The solubility of ARP was highest with stearic acid (20 \pm 5.24 mg/mL) as compared to other lipids

Table 3: Evaluation of ARP loaded NLCs.

| Formulation Code | Particle Size (nm) (Y_1) | Entrapment Efficiency (%) (Y_2) | % Cumulative Drug Release (Y_3) |
|------------------|------------------------------|-------------------------------------|-------------------------------------|
| Z1 | 211.12±2.10 | 80.21±0.98 | 60.32±0.96 |
| Z2 | 266.23±3.21 | 71.91±1.25 | 58.11±1.26 |
| Z3 | 295.13±5.02 | 64.69±1.63 | 54.62±1.09 |
| Z4 | 164.02±1.21 | 91.15±1.02 | 68.53±0.36 |
| Z5 | 192.12±4.23 | 85.67±1.62 | 64.85±0.98 |
| Z6 | 244.05±3.02 | 77.24±0.79 | 62.58±1.34 |
| Z7 | 150.46±2.24 | 93.41±1.34 | 75.45±1.22 |
| Z8 | 177.34±3.52 | 90.11±2.13 | 72.15±1.01 |
| Z9 | 252.08±4.81 | 74.72±1.74 | 70.23±0.63 |

All values are expressed in \pm SD ($n=3$).

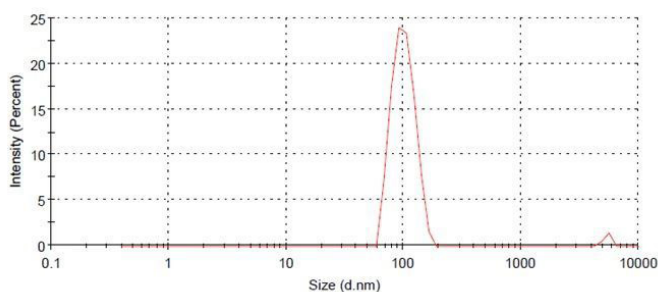


Figure 1: Frequency distribution curve of aripiprazole loaded NLC formulation (Z7).

tested (carnauba wax ~15 mg/mL and glyceryl monostearate ~18 mg/mL). Hence, stearic acid was identified as a solid lipid. Stearic acid is a saturated fatty acid with an 18-carbon chain and has been widely used in developing NLCs including intranasal delivery.^{47,48} The ARP presented the highest solubility in castor oil (68±4.23 mg/mL) followed by oleic acid (~63 mg/mL) and paraffin oil (~59 mg/mL) and thus castor oil was selected as a liquid lipid for the preparation NLCs. The concentrations (1-3%) of Tween 80 used here based on the literature.³³

Development of ARP Loaded NLCs

Various batches of formulation were effectively developed by using the high speed homogenization technique. The influence of solid/liquid lipids and surfactant in the physicochemical properties of NLCs is well documented,⁴⁹ hence were considered as independent variables. Various parameters were studied such as the size of particles, efficiency of entrapment, and ARP release on all of the formulations and the results are depicted in Table 3.

Data Analysis for Particle Size

The respective polynomial equations were created to show the link between the levels of independent variables and observed responses. The response changes that occur when two aspects are concurrently altered are represented by the interaction terms (X_1X_2). To explore non-linearity, the polynomial terms ($X_1^2X_2^2$)

are added. The physical stability, solubility, release kinetics as well as biological activity of the NLC is significantly influenced by the size of the particles.⁵⁰ The ARP loaded NLCs ranged in particle size from 150 nm to 295 nm, with Z3 having the biggest particle size, while Z7 had the smallest particle size (Figure 1), followed by Z4, which demonstrates the strong influence of the independent factors on the size of NLCs. The proportion of solid to liquid lipid displayed a negative effect (i.e. increment) on the size of NLCs according to the polynomial equation below.

$$\text{Particle size } (Y_1) = 216.78 - 41.78X_1 - 5.11X_1^2 + 40.56X_2 - 16.78X_2^2 - 4.56X_1X_2 + 13.78X_1^2X_2 + 5.78X_1X_2^2 - 2.89X_1^2X_2^2$$

The negative effect suggests that the higher the ratio of solid lipids, the greater the particle hydrodynamic size of the NLCs. This observation also agrees with the results of earlier studies.⁴⁹ The size of NLCs responded favorably to Tween 80 concentration. The positive symbol denotes that enhancement in the concentration of Tween 80 causes a decline in the NLC size because it decreases the interfacial tension that exists at the water/lipid interface, which further results in the production of tiny emulsion particles.⁵¹ Thus, adding more concentration of surfactant to the NLC system will successfully stabilize the particles and stop coalescence.⁵²

Data Analysis for Entrapment Efficiency

As seen in Table 3, the entrapment efficiency of ARP in the prepared nanoparticles varied between 64.69% to 93.41%. The values presented here confirmed that the entrapment efficiency of ARP loaded NLCs was significantly influenced by the independent factors used. The highest entrapment was found in formulation Z7 whereas formulation Z3 presented the least entrapment efficiency (Table 3). The polynomial equation clearly indicates that an increase in the quantity of lipid ratio had an opposite effect on the entrapment efficiency i.e. decrease in the entrapment efficiency. However, the quantity of surfactant increased had a progressive effect i.e. enhances the entrapment efficiency. This enhancement could be related to the effect of the

increase in surfactant content decreases the particle size, which then increases the entrapment efficiency of the NLCs.²⁸

$$\% \text{ Entrapment Efficiency } (Y_2) = 81.01 + 7.24X_1 + 1.55X_1^2 - 8.74X_2 + 3.67X_2^2 + 0.6956X_1X_2 - 1.91X_1^2X_2 - 0.7811X_1X_2^2 - 0.5678X_1^2X_2^2$$

Data Analysis for *in vitro* Release

The % CDR was determined from the observed *in vitro* drug release profiles of Z1-Z9 NLCs (Figure 2). The CDR ranged from 54.62% to 75.45% as mentioned in Table 3. NLC Z7 had the highest CDR of 75.45%, owing to the particle compact size and high entrapment value. The lipid ratio presented an insignificant result on the drug release, however, the increase in the amount of Tween 80 shown a positive effect, according to the polynomial equation observed below.

$$\% \text{ CDR } (Y_3) = 65.20 + 2.90X_1 - 0.1678X_1^2 - 7.52X_2 + 0.1156X_2^2 - 0.2589X_1X_2 + 0.5944X_1^2X_2 + 0.3144X_1X_2^2 - 0.3022X_1^2X_2^2$$

A rise in the Tween 80 levels resulted in an enhancement in the drug release pattern. This observation is due to the lower particle size and higher drug entrapment in the NLCs. The ARP release from all the prepared NLCs (Z1-Z9) shown a biphasic pattern, meaning that the drug was initially on the surface of the NLC, assisting in quick release and subsequently a steady release from the drug core (Figure 2).

To verify the linearity of the release profile and pinpoint the drug release kinetics mechanism, the CDR from the prepared NLCs was fitted into a variety of release kinetic models that include zero, first order, Korsmeyer-Peppas and Higuchi.⁴⁰ The Higuchi model which depicts the biphasic drug release from the NLCs, was deemed to be the best fitted model since it had the highest coefficient of determination (r^2) as presented in Table 4. This observation is in agreement with an earlier study wherein it was described that the release mechanism of drugs from this type of vesicles generally by diffusion.⁵³

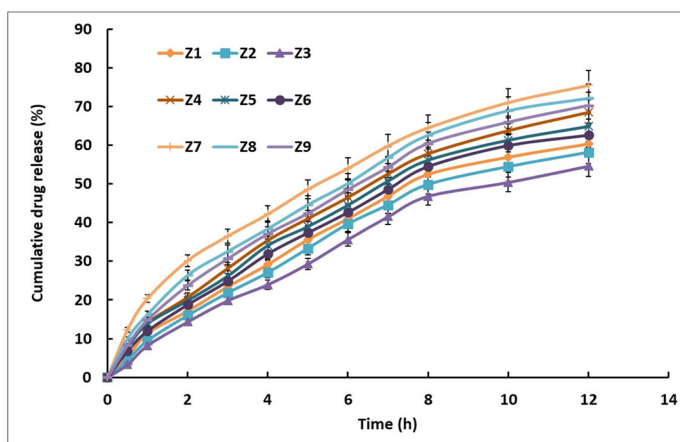


Figure 2: Percentage cumulative drug release of prepared NLCs (Z1-Z9). All values are expressed in \pm SD ($n=3$).

Response- Surface Analysis

Figure 3 shows the three-dimensional response surface plots that were created for the ARP loaded NLCs graphic optimization. Enlargement in the particle size of NLCs was noticed with the increment in the solid lipid while it was the opposite with the increase in the Tween 80 amount. The maximum entrapment efficiency was observed at the highest level of surfactant amount (3%) and low levels of solid lipid and liquid lipid ratio (1:1). Nevertheless, the highest drug release was observed at the highest level of Tween 80, while the lipid ratio has negligible effect. NLC Z7 had the lowest particle size (\sim 150 nm), the highest percentage of cumulative drug release (\sim 75.45%) and the entrapment efficiency (\sim 93.41 of all the formulations tested). Thus, the formulation Z7 was chosen as the optimized preparation and the selected NLC was incorporated into the *in situ* gel.

DSC

The nature of ARP in NLCs was determined with the help of DSC. Figure 4 presents the analysis of the thermograms of pure ARP and optimized NLC (Z7). As demonstrated in the thermogram (Figure 4a) of ARP, there was a pronounced heat absorbing peak at 149.94°C, which represents the melting point of the drug. The observed sharp peak signifies the crystalline nature of pure ARP. However, the thermogram of ARP loaded NLCs revealed a shifting of peak to a lower temperature at 59.85°C (stearic acid) and 132.60°C (ARP) as well as a decline in the enthalpies in Z7 (Figure 4b). The possible explanation for the shifting of the endothermic peak (in Z7 NLC) is an indication of the formation of the NLC matrix during the heating of APR with molten excipients, resulting in a reduction in crystallinity, as reported in the literature.^{47,48}

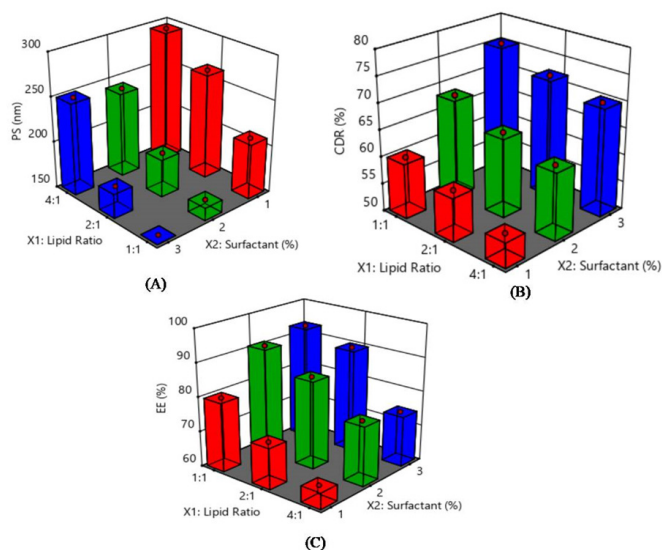


Figure 3: 3D plots displaying the influence of solid and liquid lipid ratio (X_1) and concentration of surfactant (X_2), on particle size (A), % cumulative drug release (B) and % entrapment efficiency (C).

Table 4: Correlation coefficient (r_2) values observed in release kinetics of ARP loaded NLCs.

| Formulation Code | Zero Order Model | First order Model | Higuchi Model | Korsmeyer-Peppas Model |
|------------------|------------------|-------------------|---------------|------------------------|
| Z1 | 0.922 | 0.520 | 0.994 | 0.560 |
| Z2 | 0.920 | 0.518 | 0.992 | 0.559 |
| Z3 | 0.919 | 0.517 | 0.991 | 0.556 |
| Z4 | 0.924 | 0.522 | 0.995 | 0.562 |
| Z5 | 0.922 | 0.520 | 0.993 | 0.560 |
| Z6 | 0.921 | 0.519 | 0.992 | 0.558 |
| Z7 | 0.927 | 0.524 | 0.996 | 0.563 |
| Z8 | 0.925 | 0.522 | 0.994 | 0.558 |
| Z9 | 0.921 | 0.518 | 0.990 | 0.554 |

Table 5: Stability study data of ARP loaded NLCs (Z7).

| Time (days) | Physical Change | Particle size (nm) | Entrapment Efficiency (%) | % CDR at 12 hr |
|-------------|-----------------|--------------------|---------------------------|----------------|
| 0 | No change | 150 ±1.20 | 93.41±1.34 | 75.45±1.22 |
| 30 | No change | 155±0.56 | 93.06±0.96 | 75.01±0.64 |
| 60 | No change | 163±0.42 | 92.41±0.87 | 74.29±0.47 |
| 90 | No change | 171±1.33 | 90.06±1.52 | 73.17±0.35 |

All values are expressed in \pm SD ($n=3$).

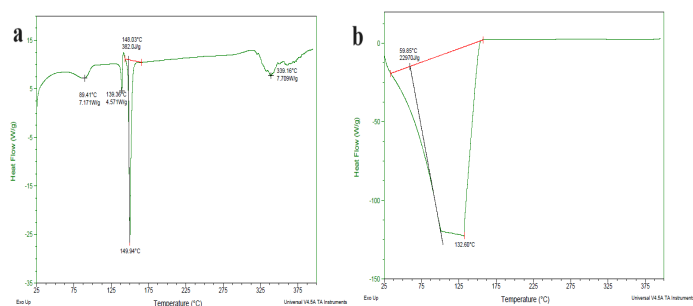


Figure 4: DSC thermogram of aripiprazole (a) and optimized (Z7) aripiprazole loaded NLC (b).

TEM

The use of TEM has become essential for characterizing vesicular drug delivery system architectures. It can be used to investigate the general colloidal composition of the associated dispersions as well as the size and shape of colloidal carriers.⁵⁴ As demonstrated in the TEM image of Z7, the particles are spherical in shape (Figure 5). The sizes of the NLCs were less than 200 nm, which indicates that the prepared vesicles are ideal for intranasal administration. In addition, particles are uniform in size and distributed evenly.

ARP loaded NLCs Thermoreversible *in situ* Gel Formulation

The optimized ARP loaded NLC preparation (Z7) was subsequently incorporated in an *in situ* gelling system in order to produce better regulated drug release from the gelling system

(Z1 G to Z6 G) using a direct dispersion approach. Indeed one of the goals of the current investigation was to create a dosage that would exhibit phase change at the nasal cavity temperature. Poloxamer 407 (25% w/v) was used as a phase transition catalyst, and the drug level was fixed at 2% in the thermoreversible *in situ* gel. Carbopol 940P or PVP K30 in the concentration of 0.2-0.6% w/v were utilised as mucoadhesive agents. Poloxamer 407 solutions exhibit the phase transition (conversion of sol to gel) at temperatures below 36°C. The phase change may cause difficulties in handling the formulations at temperatures lower than 27°C. On the other hand, if the gelation temperature is more than 36°C, the main problem is the leakage of medication from the nasal cavity. For the formulation of *in situ* gels, batches showing the sol to gel phase transition in the range of 25-32°C are ideal for nostril application.

Evaluation of ARP loaded NLCs Gel

The effects of the selected mucoadhesive polymers (carbopol 940 and PVP K30) with poloxamer 407 (25% w/v) on gelling temperature, gel strength, and pH were examined using *in situ* gels (Z1 G to Z6 G). The observed pharmaceutical characteristics are presented in Figure 6. The data in the Figure 6 shows that when the amount of mucoadhesive agents increased, the gelation temperature reduced (35.2 to 27.1°C). A similar observation was noticed with gel strength as well. Further, the pH of the developed formulations was comparable. It was observed that the pH of the Z2 G gel was 6.3, which is suitable and nonirritant to nasal

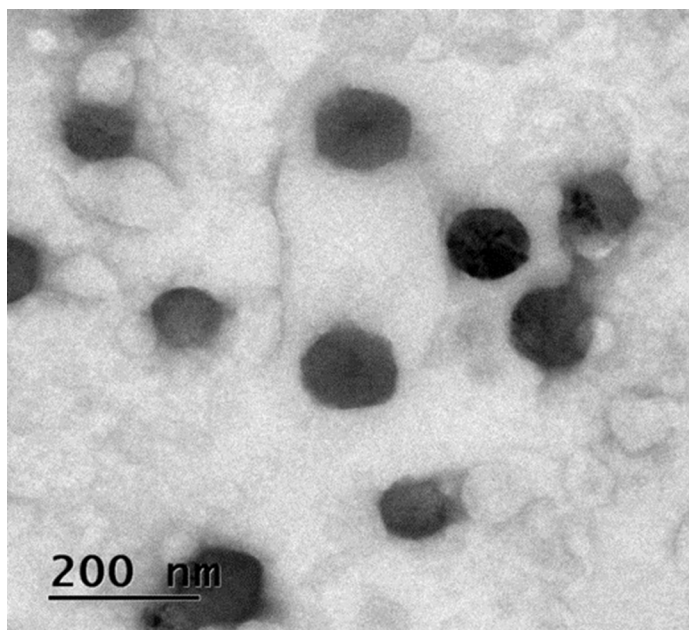


Figure 5: TEM image of optimized aripiprazole loaded nanostructured lipid carrier (Z7).

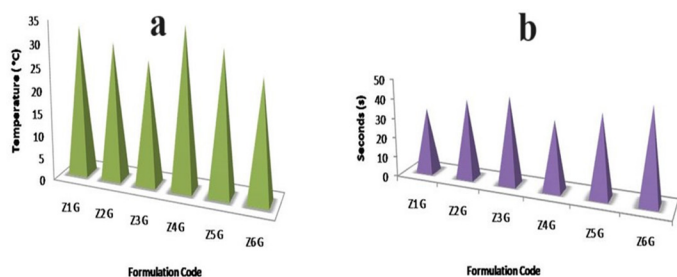


Figure 6: Gelling temperature (a) and gel strength (b) of *in situ* intranasal gels.

physiological conditions as the nasal mucosa's pH normally ranges between 5.5 to 6.5.⁵⁵ As the optimal gel strength is considered as in the range of 33–47 s and gelling temperature around 30°C, the *in situ* gel (Z2 G) which showed ideal characteristics was regarded as the optimized formulation.

Ex vivo Drug Permeation Studies

The permeability of selected NLC *in situ* gel (Z2 G) and the control was determined by diffusion experiments using goat mucosa membrane. Comparative permeation profiles of ARP loaded NLC thermoreversible *in situ* gel and pure drug suspension (control) are presented in Figure 7. The permeation profile noticed here with NLC gel indicates the permeation seems to be rapid and steady with time and visibly different from the control. It can be seen that ARP loaded NLCs showed a greater permeation ($p < 0.0001$) of ~60% in 12 hr while the pure drug suspension showed a permeation of ~30%. The greater flux observed here indicates the ARP loaded NLC gel is capable of permeating the nasal mucosa with ease. Meanwhile, the low permeation of ARP from control is probably because of its low solubility/permeability as similar results were noticed in a recent study.³

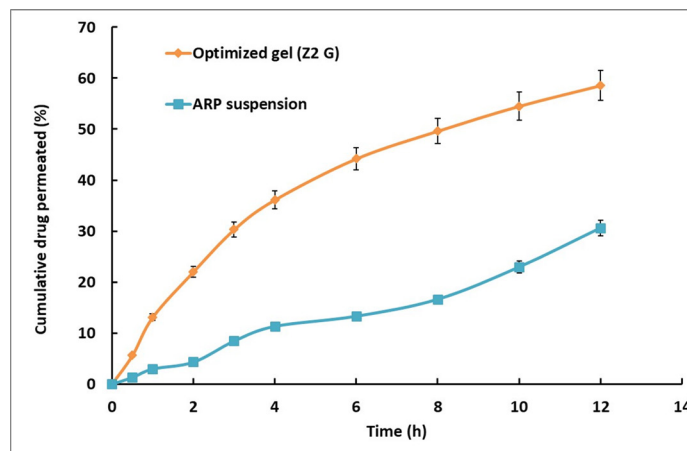


Figure 7: Permeation profile of pure drug suspension and ARP loaded NLC thermoreversible *in situ* gel (Z2 G) through goat nasal membrane.

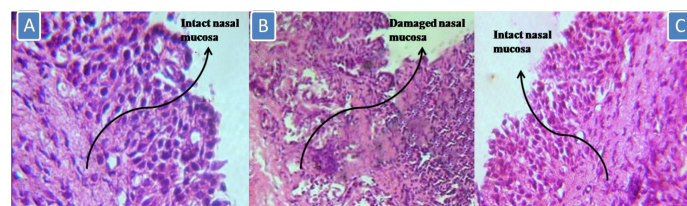


Figure 8: Nasal histopathological studies A) negative control, no nasal treatment B) positive control, treated with isopropyl alcohol and C) treated with ARP loaded NLC *in situ* gel.

Histopathological Studies

Histopathological analysis was performed by comparing the nasal mucosal membranes of untreated and treated groups to check the histological variations that happened due to the application of developed *in situ* gel formulation (Z2 G). Figure 8 shows histopathological pictures of treatments used in investigations on nasal ciliotoxicity studies. The test sample (Figure 8C) treated with ARP loaded NLC *in situ* gel (Z2 G) and the positive control (isopropyl alcohol treated nasal mucosa, Figure 8B) were compared with microscopic images of the untreated nasal mucosa (negative control, Figure 8A). Figure 8C demonstrates that the epithelial layer has not been damaged or removed in comparison to the normal mucosa (Figure 8A), confirms no substantial histological change has taken place and reiterates the safety of intranasal administration of developed nasal gel. However, Figure 8B, in contrast to Figures 8A and C, demonstrates complete necrosis of nasal mucosa cells following mucociliary toxic agent treatment. This result signifies the nontoxicity of the developed formulation as described in similar investigations.^{29,30}

Stability Studies

Table 5 summarizes the stability results of optimized NLCs (Z7) stored at $25 \pm 2^\circ\text{C}$ temperature and $60 \pm 5\%$ relative humidity for three months. Indeed, no visible physical changes were observed. However, there was a minor enlargement in the particle size during the 3 months of storage. The entrapment efficiency and % CDR were found to decrease marginally.

CONCLUSION

A thermoreversible *in situ* gel with ARP loaded NLCs was successfully developed for intranasal delivery to increase the solubility and bioavailability. ARP loaded NLCs were developed using the high speed homogenization technique and optimization was carried out by selecting independent variables and assessing their effect on response. The optimized NLCs were formulated into *in situ* gel. The data observed here indicates that the prepared NLCs showed a steady release of ARP and enhanced flux through the nasal mucosal membrane. The absence of ciliotoxicity in the improved formulation indicates that the components used in this investigation are safe for the nasal mucosa. The findings of this study suggested that using thermoreversible *in situ* gel incorporating drug loaded NLC is a successful approach for delivering ARP to the brain through the intranasal route.

ACKNOWLEDGEMENT

This work was supported by the Deanship of Scientific Research, Vice-Presidency for Graduate Studies and Scientific Research, King Faisal University, Saudi Arabia.

FUNDING

This work was supported through the Empowered Female Researcher track by the Deanship of Scientific Research, Vice Presidency for Graduate Studies and Scientific Research, King Faisal University, Saudi Arabia [Project No. GRANT5593].

CONFLICT OF INTEREST

The authors declare that there is no conflict of interest.

REFERENCES

- Baker JT, Holmes AJ, Masters GA, Yeo BT, Krienen F, Buckner RL, et al. Disruption of cortical association networks in schizophrenia and psychotic bipolar disorder. *JAMA Psychiatry*. 2014; 71(2): 109-18. doi: 10.1001/jamapsychiatry.2013.3469, PMID 24306091.
- Joseph J, Hari Sankar D, Nambiar D. The burden of mental health illnesses in Kerala: a secondary analysis of reported data from 2002 to 2018. *BMC Public Health*. 2021; 21(1): 2264. doi: 10.1186/s12889-021-12289-0, PMID 34895187.
- Kumbhar SA, Kokare CR, Shrivastava B, Gorain B, Choudhury H. Antipsychotic potential and safety profile of TPGS-based mucoadhesive aripiprazole nanoemulsion: development and optimization for nose-to-brain delivery. *J Pharm Sci*. 2021; 110(4): 1761-78. doi: 10.1016/j.xphs.2021.01.021, PMID 33515583.
- Stępnicki P, Kondej M, Kaczor AA. Current concepts and treatments of schizophrenia. *Molecules*. 2018; 23(8): 2087. doi: 10.3390/molecules23082087, PMID 30127324.
- Fellner C. New schizophrenia treatments address unmet clinical needs. *P T*. 2017; 42(2): 130-4. PMID 28163559.
- Granger KT, Sand M, Caswell S, Lizarraga-Valderrama LR, Barnett JH, Moran PM. A new era for schizophrenia drug development - Lessons for the future. *Drug Discov Today*. 2023; 28(7): 103603. doi: 10.1016/j.drudis.2023.103603, PMID 37142156.
- Fabrazzo M, Cipolla S, Camerlengo A, Perris F, Catapano F. Second-generation antipsychotics' effectiveness and tolerability: a review of real-world studies in patients with schizophrenia and related disorders. *J Clin Med*. 2022; 11(15):4530. doi: 10.3390/jcm11154530, PMID 35956145.
- Preda A, Shapiro BB. A safety evaluation of aripiprazole in the treatment of schizophrenia. *Expert Opin Drug Saf*. 2020; 19(12): 1529-38. doi: 10.1080/14740338.2020.1832990, PMID 33064050.
- de Bartolomeis A, Tomasetti C, Iasevoli F. Update on the mechanism of action of aripiprazole: translational insights into antipsychotic strategies beyond dopamine receptor antagonism. *CNS Drugs*. 2015; 29(9): 773-99. doi: 10.1007/s40263-015-0278-3, PMID 26346901.

- Ardiana F, Lestari ML, Indrayanto G. Aripiprazole. *Profiles Drug Subst Excipients Relat Methodol*. 2013; 38: 35-85.
- Sawant K, Pandey A, Patel S. Aripiprazole loaded poly(ϵ -caprolactone) nanoparticles: optimization and *in vivo* pharmacokinetics. *Mater Sci Eng C Mater Biol Appl*. 2016; 66: 230-43. doi: 10.1016/j.msec.2016.04.089, PMID 27207059.
- Silki SVR, Sinha VR. Enhancement of *in vivo* efficacy and oral bioavailability of aripiprazole with solid lipid nanoparticles. *AAPS PharmSciTech*. 2018; 19(3): 1264-73. doi: 10.1208/s12249-017-0944-5, PMID 29313261.
- Zhou Q, Tan Z, Yang D, Tu J, Wang Y, Zhang Y, et al. Improving the solubility of aripiprazole by multicomponent crystallization. *Crystals*. 2021; 11(4): 343. doi: 10.3390/cryst11040343.
- Jawahar N, Hingarh PK, Arun R, Selvaraj J, Anbarasan A, S S, et al. Enhanced oral bioavailability of an antipsychotic drug through nanostructured lipid carriers. *Int J Biol Macromol*. 2018; 110: 269-75. doi: 10.1016/j.ijbiomac.2018.01.121, PMID 29402457.
- Łyszczarz E, Hofmanová J, Szafraniec-Szczyński J, Jachowicz R. Orally dispersible films containing ball milled aripiprazole-polyoxamer[®]407 solid dispersions. *Int J Pharm*. 2020; 575: 118955. doi: 10.1016/j.ijpharm.2019.118955, PMID 31843552.
- Ferreira MD, Duarte J, Veiga F, Paiva-Santos AC, Pires PC. Nanosystems for brain targeting of antipsychotic drugs: an update on the most promising nanocarriers for increased bioavailability and therapeutic efficacy. *Pharmaceutics*. 2023; 15(2):678. doi: 10.3390/pharmaceutics15020678, PMID 36840000.
- Pinheiro RGR, Coutinho AJ, Pinheiro M, Neves AR. Nanoparticles for targeted brain drug delivery: what do we know? *Int J Mol Sci*. 2021; 22(21):11654. doi: 10.3390/ijms222111654, PMID 34769082.
- Ahlatwaj J, Guillama Barroso G, Masoudi Asil S, Alvarado M, Armendariz I, Bernal J, et al. Nanocarriers as potential drug delivery candidates for overcoming the blood-brain barrier: challenges and possibilities. *ACS Omega*. 2020; 5(22): 12583-95. doi: 10.1021/acsomega.0c01592, PMID 32548442.
- Kamboj S, Bala S, Nair AB. Solid lipid nanoparticles: an effective lipid based technology for poorly water soluble drugs. *Int J Pharm Sci Rev Res*. 2010; 5(2): 78-90.
- Kotta S, Aldawsari HM, Badr-Eldin SM, Nair AB, Yt K. K. Progress in polymeric micelles for drug delivery applications. *Pharmaceutics*. 2022; 14(8). doi: 10.3390/pharmaceutics14081636, PMID 36015262.
- Trevino JT, Quispe RC, Khan F, Novak V. Non-invasive strategies for nose-to-brain drug delivery. *J Clin Trials*. 2020; 10(7). PMID 33505777.
- Jeong SH, Jang JH, Lee YB. Drug delivery to the brain via the nasal route of administration: exploration of key targets and major consideration factors. *J Pharm Invest*. 2023; 53(1): 119-52. doi: 10.1007/s40005-022-00589-5, PMID 35910081.
- Bhandari M, Shah J, Gorain B, Nair AB, Jacob S, Asdaq SMB, et al. Optimized rivastigmine nanoparticles coated with Eudragit for intranasal application to brain delivery: evaluation and nasal ciliotoxicity studies. *Materials (Basel, Switzerland)*. 2021; 14(21):6291. doi: 10.3390/ma14216291, PMID 34771817.
- Costa CP, Moreira JN, Sousa Lobo JM, Silva AC. Intranasal delivery of nanostructured lipid carriers, solid lipid nanoparticles and nanoemulsions: A current overview of *in vivo* studies. *Acta Pharm Sin B*. 2021; 11(4): 925-40. doi: 10.1016/j.apsb.2021.02.012, PMID 33996407.
- Ahmad J, Rizwanullah M, Amin S, Warsi MH, Ahmad MZ, Barkat MA. Nanostructured lipid carriers (NLCs): nose-to-brain delivery and theranostic application. *Curr Drug Metab*. 2020; 21(14): 1136-43. doi: 10.2174/1389200221666200719003304, PMID 32682366.
- Taha E, Nour SA, Mamdouh W, Selim AA, Swidan MM, Ibrahim AB, et al. Cod liver oil nano-structured lipid carriers (Cod-NLCs) as a promising platform for nose to brain delivery: preparation, *in vitro* optimization, *ex vivo* cytotoxicity & *in vivo* biodistribution utilizing radiolabeled zopiclone. *Int J Pharm X*. 2023; 5: 100160. doi: 10.1016/j.ijpx.2023.100160, PMID 36647457.
- Jacob S, Nair AB, Shah J, et al. Lipid nanoparticles as a promising drug delivery carrier for topical ocular therapy-an overview on recent. *Adv Pharm*. 2022; 14(3):533.
- Viegas C, Patrício AB, Prata JM, Nadhman A, Chintamaneni PK, Fonte P. Solid Lipid Nanoparticles vs. nanostructured Lipid Carriers: A Comparative Review. *Pharmaceutics*. 2023; 15(6):1593. doi: 10.3390/pharmaceutics15061593, PMID 37376042.
- Nair AB, Chaudhary S, Shah H, Jacob S, Mewada V, Shinu P, et al. Intranasal Delivery of Darunavir-Loaded mucoadhesive *in situ* Gel: experimental Design, *in vitro* Evaluation, and pharmacokinetic Studies. *Gels*. 2022; 8(6):342. doi: 10.3390/gels8060342, PMID 35735686.
- Nair AB, Chaudhary S, Jacob S, Patel D, Shinu P, Shah H, et al. Intranasal Administration of Dolutegravir-Loaded nanoemulsion-Based *in situ* Gel for Enhanced Bioavailability and Direct Brain Targeting. *Gels*. 2023; 9(2):130. doi: 10.3390/gels9020130, PMID 36826300.
- Corazza E, di Cagno MP, Bauer-Brandl A, Abruzzo A, Cerchiara T, Bigucci F, et al. Drug delivery to the brain: *in situ* gelling formulation enhances carbamazepine diffusion through nasal mucosa models with mucin. *Eur J Pharm Sci*. 2022; 179: 106294. doi: 10.1016/j.ejps.2022.106294, PMID 36116696.
- Mahmood A, Rapalli VK, Gorantla S, Waghule T, Singhvi G. Dermatokinetic assessment of luliconazole-loaded nanostructured lipid carriers (NLCs) for topical delivery: QbD-driven design, optimization, and *in vitro* and *ex vivo* evaluations. *Drug Deliv Transl Res*. 2022; 12(5): 1118-35. doi: 10.1007/s13346-021-00986-7, PMID 33895936.

33. AlMulhim FM, Nair AB, Aldhubiab B, Shah H, Shah J, Mewada V, *et al.* Design, development, evaluation, and *in vivo* performance of buccal films embedded with paliperidone-loaded nanostructured lipid carriers. *Pharmaceutics*. 2023;15(11):2530. doi: 10.3390/pharmaceutics15112530, PMID 38004510.
34. Gomaa E, Fathi HA, Eissa NG, Elsbahy M. Methods for preparation of nanostructured lipid carriers. *Methods*. 2022; 199: 3-8. doi: 10.1016/j.ymeth.2021.05.003, PMID 33992771.
35. Kumar M, Tiwari A, Asdaq SMB, Nair AB, Bhatt S, Shinu P, *et al.* Itraconazole loaded nano-structured lipid carrier for topical ocular delivery: optimization and evaluation. *Saudi J Biol Sci*. 2022; 29(1): 1-10. doi: 10.1016/j.sjbs.2021.11.006, PMID 35002390.
36. Subramaniam B, Siddik ZH, Nagoor NH. Optimization of nanostructured lipid carriers: understanding the types, designs, and parameters in the process of formulations. *J Nanopart Res*. 2020; 22: 1-29.
37. Nair AB, Shah J, Al-Dhubiab BE, Patel SS, Morsy MA, Patel V, *et al.* Development of asialoglycoprotein receptor-targeted nanoparticles for selective delivery of gemcitabine to hepatocellular carcinoma. *Molecules*. 2019; 24(24): 4566. doi: 10.3390/molecules24244566, PMID 31847085.
38. Pandey SS, Shah KM, Maulvi FA, Desai DT, Gupta AR, Joshi SV, *et al.* Topical delivery of cyclosporine loaded tailored niosomal nanocarriers for improved skin penetration and deposition in psoriasis: optimization, *ex vivo* and animal studies. *J Drug Deliv Sci Technol*. 2021; 63: 102441. doi: 10.1016/j.jddst.2021.102441.
39. Shete MB, Deshpande AS, Shende P. Enhancement of *in vitro* anti-oral cancer activities of silymarin using dispersion of nanostructured lipid carrier in mucoadhesive *in situ* gel. *Int J Pharm*. 2023; 636: 122860. doi: 10.1016/j.ijpharm.2023.122860, PMID 36933584.
40. Nair A, Gupta R, Vasanti S. *In vitro* controlled release of alfuzosin hydrochloride using HPMC-based matrix tablets and its comparison with marketed product. *Pharm Dev Technol*. 2007; 12(6): 621-5. doi: 10.1080/10837450701563277, PMID 18161635.
41. Choi H-G, Oh Y-K, Kim C-K. *In situ* gelling and mucoadhesive liquid suppository containing acetaminophen: enhanced bioavailability. *Int J Pharm*. 1998;165(1):23-32. doi: 10.1016/S0378-5173(97)00385-2.
42. Naresh WR, Dilip DV, Sunil KP. Xyloglucan based nasal *in situ* gel formulation of mirtazapine for treatment of depression. *Indian J Pharm Educ Res*. 2020; 54:s210-9.
43. Anroop B, Ghosh B, Parcha V, Kumar A, Khanam J. Synthesis and comparative skin permeability of atenolol and propranolol esters. *J Drug Deliv Sci Technol*. 2005; 15(2): 187-90. doi: 10.1016/S1773-2247(05)50025-X.
44. Guideline IHT. Stability testing of new drug substances and products. current step. 2003; 4:Q1A (R2):1-24.
45. Sabale V, Jiwankar M. Nanostructured lipid carriers in chemotherapeutics: an overview. *Ind J Pharm Educ Res*. 2023; 57(2): 310-9. doi: 10.5530/ijper.57.2.40.
46. Tetyczka C, Griesbacher M, Absenger-Novak M, Fröhlich E, Roblegg E. Development of nanostructured lipid carriers for intraoral delivery of domperidone. *Int J Pharm*. 2017; 526(1-2): 188-98. doi: 10.1016/j.ijpharm.2017.04.076, PMID 28461264.
47. Matarazzo AP, Elisei LMS, Carvalho FC, Bonfilio R, Ruela ALM, Galdino G, *et al.* Mucoadhesive nanostructured lipid carriers as a cannabidiol nasal delivery system for the treatment of neuropathic pain. *Eur J Pharm Sci*. 2021; 159: 105698. doi: 10.1016/j.ejps.2020.105698, PMID 33406408.
48. Mohanty D, Alsaidan OA, Zafar A, Doodle T, Gupta JK, Yasir M, *et al.* Development of atomoxetine-Loaded NLC *in situ* Gelfor Nose-to-Brain Delivery: optimization, *in vitro*, and Preclinical Evaluation. *Pharmaceutics*. 2023;15(7):1985. doi: 10.3390/pharmaceutics15071985, PMID 37514171.
49. Apostolou M, Assi S, Fatokun AA, Khan I. The effects of solid and liquid lipids on the physicochemical properties of nanostructured lipid carriers. *J Pharm Sci*. 2021; 110(8): 2859-72. doi: 10.1016/j.xphs.2021.04.012, PMID 33901564.
50. Khosa A, Reddi S, Saha RN. Nanostructured lipid carriers for site-specific drug delivery. *Biomed Pharmacother*. 2018; 103: 598-613. doi: 10.1016/j.biopha.2018.04.055, PMID 29677547.
51. Witayaudom P, Klinkensorn U. Effect of surfactant concentration and solidification temperature on the characteristics and stability of nanostructured lipid carrier (NLC) prepared from rambutan (*Nephelium lappaceum* L.) kernel fat. *J Colloid Interface Sci*. 2017; 505: 1082-92. doi: 10.1016/j.jcis.2017.07.008, PMID 28697547.
52. Sakellari GI, Zafeiri I, Batchelor H, Spyropoulos F. Solid lipid nanoparticles and nanostructured lipid carriers of dual functionality at emulsion interfaces. Part I: Pickering stabilisation functionality. *Colloids Surf A Physicochem Eng Aspects*. 2022; 654: 130135. doi: 10.1016/j.colsurfa.2022.130135.
53. Kraisit P, Sarisuta N. Development of triamcinolone acetanide-loaded nanostructured lipid carriers (NLCs) for buccal drug delivery using the Box-Behnken design. *Molecules*. 2018; 23(4):982. doi: 10.3390/molecules23040982, PMID 29690622.
54. Kuntsche J, Horst JC, Bunjes H. Cryogenic transmission electron microscopy (cryo-TEM) for studying the morphology of colloidal drug delivery systems. *Int J Pharm*. 2011; 417(1-2): 120-37. doi: 10.1016/j.ijpharm.2011.02.001, PMID 21310225.
55. Keller LA, Merkel O, Popp A. Intranasal drug delivery: opportunities and toxicologic challenges during drug development. *Drug Deliv Transl Res*. 2022; 12(4): 735-57. doi: 10.1007/s13346-020-00891-5, PMID 33491126.

Cite this article: Albaqshi L, Singh A, Khan S, Kumar M, Kour J, Pottathil S, *et al.* Formulation and Optimization of Aripiprazole-Loaded Nanostructured Lipid Carriers for Nose-to-Brain Delivery. *Indian J of Pharmaceutical Education and Research*. 2024;58(2):579-88.